Robotica (2000) volume 18, pp. 369–374. Printed in the United Kingdom © 2000 Cambridge University Press

Tracking adaptive impedance robot control with visual feedback

Vicente Mut, Oscar Nasisi, Ricardo Carelli and Benjamín Kuchen

Instituto de Automática, Universidad Nacional de San Juan, San Juan 5400 (Argentina)
e-mail: vmut@inaut.unsj.edu.ar

(Received in Final Form: November 10, 1999)

SUMMARY

In this paper we propose a tracking adaptive impedance controller for robots with visual feedback. It is based on a generalized impedance concept where the sensed distance is introduced as a fictitious force to the control in order to avoid obstacles in restricted motion tasks. The controller is designed to compensate for full non-linear robot dynamics. Robot parameters adjustment is introduced to reduce the sensibility of the controller design to dynamic uncertainties of the robot and the manipulated load. It is proved that the vision control errors are ultimately bounded in the image coordinate system. Simulations are carried out to evaluate the controller performance.

KEYWORDS: Robot control; Visual feedback; Adaptive impedance; Image system.

1. INTRODUCTION

The automation of tasks in the industry, those in which the robot interacts with the environment, needs the incorporation of sensors and the generation of control strategies which use this sensory information. Among controllers for constrained robot motion, impedance control[1] is designed to regulate the manipulator's mechanical impedance, that is the dynamic relationship between the applied force and the motion error. Force sensors are required for sensing the interaction force.

The present work is related to the generalized impedance robot control using visual feedback in which a strategy of adaptive control is presented to deal with the problem of uncertainties in the manipulator's dynamics. Previous work[2] considered the concept of elasticity related to the distance sensing. In this work, the concept of impedance is generalized and the sensed distance is introduced like a fictitious force to the impedance control. The distance is assumed to be measured by means of the vision sensor. The tasks of the robotic manipulator with constrained motion can be classified into: with contact (force sensor) and without contact (distance sensor). Tasks without contact are emphasized, the first ones being reserved for the robot's eventual mechanical contacts with the environment. In tasks without contact, attractive surfaces (e.g. useful for profiles tracking) and refractory surfaces (e.g. to avoid obstacles) can be generated.

The use of visual information in the feedback loop represents an attractive solution to motion control of autonomous manipulators evolving in unstructured environments. In this context, motion robot control uses direct visual sensory information to achieve a desired relative position between the robot and –possible moving– object in the robot environment. Some solutions to this problem have been proposed[3,4] in which non-linear robot dynamics has not been considered for the controller design. These controllers can result in unsatisfactory control under high performance requirements, including high speed tasks and direct-drive robot actuators. In such cases, the robot dynamics has to be considered in the controller design, as partially done in reference [5] or fully including in reference [6]. These schemes assume an exact knowledge of robot dynamics, and may result, in general, to be sensitive to robot model uncertainties as is presented in reference [7].

This paper presents an adaptive impedance robot controller in which signals are backfed directly from internal position and velocity sensors and visual information. The tracking impedance control errors are proved to be ultimately bounded.[8] The controller is based on inverse dynamics, the definition of a manifold in the error space,[9] a desired impedance and a σ-modification type parameters update law. The control system proves useful to avoid obstacles when tracking an external object based on visual information.

2. DISTANCE SENSORY FEEDBACK

To regulate the robot's mechanical impedance, it is necessary to measure the interaction force in the physical contact between the robot's end effector and the environment. In some applications this contact is not desirable. This is the case of obstacle avoidance or the follow contours. The robot should react with a compliant movement when an obstacle exists in the desired motion trajectory, without causing any physical contact. This can be achieved by using the impedance control, if it is considered a fictitious force $\boldsymbol{F}$ defined as a function of the sensed distance between the end effector and the surface. For example[2] it is defined as,

$$\boldsymbol{F}=\boldsymbol{\delta k}(\boldsymbol{d}-\boldsymbol{r}) \tag{1}$$

with $\boldsymbol{\delta}=0$ if $\|\boldsymbol{d}\|>\|\boldsymbol{r}\|$ or $\boldsymbol{\delta}=1$ if $\|\boldsymbol{d}\|<\|\boldsymbol{r}\|$, where $\boldsymbol{d}$ is the sensed distance vector between the end effector and the obstacle. The distance $\boldsymbol{d}$ is calculated through an artificial vision algorithm. $\boldsymbol{k}$ is a constant with appropriate dimension and $\boldsymbol{r}\in \mathrm{IR}^n$ is a colinear vector with $\boldsymbol{d}$ representing the smaller acceptable approach from the robot to the surface. The definition given in equation (1) is adapted to develop a strategy to avoid collisions, because a refractory area is generated around the object. Other definitions of fictitious force are possible according to the particular application. For contour tracking, equation (1) should be used without the commutation function $\boldsymbol{\delta}$. This generates an appropriate fictitious force to define an attractive surface at $|\boldsymbol{r}|$ distance.

3. ROBOT AND CAMERA MODELS

In the absence of friction and other disturbances, the joint-space dynamics of an n-link manipulator can be written as,

$$\boldsymbol{H}(\boldsymbol{q})\ddot{\boldsymbol{q}}+\boldsymbol{C}\boldsymbol{q},\dot{\boldsymbol{q}})\dot{\boldsymbol{q}}+\boldsymbol{g}(\boldsymbol{q})=\boldsymbol{\tau} \quad (2)$$

where $\boldsymbol{q}$ is the $n\times 1$ vector of joint displacement, $\boldsymbol{\tau}$ is the $n\times 1$ vector of applied joint torques, $\boldsymbol{H}(\boldsymbol{q})$ is the $n\times n$ symetric positive definite manipulator inertia matrix, $\boldsymbol{C}(\boldsymbol{q},\dot{\boldsymbol{q}})\dot{\boldsymbol{q}}$ is the $n\times 1$ vector of centripetal and Coriolis torques, $\boldsymbol{g}(\boldsymbol{q})$ is the $n\times 1$ vector of gravitational torques.

The robot model (2) has some fundamental properties that can be exploited in the controller design.[10]

Property 3.1. *Using a proper definition of matrix $\boldsymbol{C}(\boldsymbol{q},\dot{\boldsymbol{q}})$ (only the vector $\boldsymbol{C}(\boldsymbol{q},\dot{\boldsymbol{q}})\dot{\boldsymbol{q}}$ is uniquely defined), matrices $\boldsymbol{H}(\boldsymbol{q})$ and $\boldsymbol{C}(\boldsymbol{q},\dot{\boldsymbol{q}})$ in (2) satisfy*

$$z^T[\frac{d}{dt}\boldsymbol{H}(\boldsymbol{q})-2\boldsymbol{C}(\boldsymbol{q},\dot{\boldsymbol{q}})]z=\boldsymbol{0}\ \forall z \in \mathbf{IR}^n \quad (3)$$

Property 3.2. *A part of the dynamic structure (2) is linear in terms of a suitably selected set of robot and load parameters, i.e.*

$$\boldsymbol{H}(\boldsymbol{q})\ddot{\boldsymbol{q}}+\boldsymbol{C}\boldsymbol{q},\dot{\boldsymbol{q}})\dot{\boldsymbol{q}}+\boldsymbol{g}(\boldsymbol{q})=\boldsymbol{\Omega}(\boldsymbol{q},\dot{\boldsymbol{q}},\ddot{\boldsymbol{q}})\theta \quad (4)$$

where $\boldsymbol{\Omega}(\boldsymbol{q},\dot{\boldsymbol{q}},\ddot{\boldsymbol{q}})$ is an $n\times p$ matrix and $\boldsymbol{\theta}$ is an $p\times 1$ vector containing the selected set of robot and load parameters.

It is assumed that the robot is equipped with joint position and velocity sensors and a vision camera mounted in the robot hand. Following reference [6], let the camera and the and the object positions be, $\boldsymbol{s}_c \in \mathrm{IR}^n$ and $\boldsymbol{s}_o \in \mathrm{IR}^{m_o}$. For an ideal perspective, the position of the object point in the image plane is,

$$\boldsymbol{\xi}=\begin{bmatrix} x \\ y \end{bmatrix}=-\boldsymbol{\alpha}\frac{f}{{}^cz_o}\begin{bmatrix} {}^cx_o \\ {}^cy_o \end{bmatrix}=i(s_c,s_o) \quad (5)$$

with f the focal length of the camera lens, $\boldsymbol{\alpha}$ is the scaling factor in *pixels/m* and $[{}^cx_o \quad {}^cy_o \quad {}^cz_o]^T$ the relative position vector of the object with respect to the camera coordinate system (${}^cz_o<0$). This model can be extended to multiple feature points of the object to obtain an extended imaging model of the camera,

$$\boldsymbol{\xi}=\boldsymbol{i}^+(s_c,s_o) \quad (6)$$

with $\boldsymbol{\xi}=[x_1y_1\ldots x_my_m]^T$.

Noting that $\boldsymbol{s}_c$ depends on $\boldsymbol{q}$, differentiating (6) it yields,

$$\dot{\boldsymbol{\xi}}=\boldsymbol{J}(\boldsymbol{q},s_o)\dot{\boldsymbol{q}}+\boldsymbol{J}_o(\boldsymbol{q},s_o)\boldsymbol{v}_o \quad (7)$$

where $\boldsymbol{J} \in \mathrm{IR}^{2m\times n}$ is the Jacobian matrix obtained as,

$$\boldsymbol{J}(\boldsymbol{q},s_o)=\boldsymbol{J}_I(s_c,s_o)\begin{bmatrix} \boldsymbol{R}_c(\boldsymbol{q}) & 0 \\ 0 & \boldsymbol{R}_c(\boldsymbol{q}) \end{bmatrix}\boldsymbol{J}_{geo}$$

where $\boldsymbol{J}_I$ is the image Jacobian matrix, $\boldsymbol{J}_{geo}$ is the geometric Jacobian matrix of the robot.[11] Also, $\boldsymbol{J}_o \in \mathrm{IR}^{2m\times m_o}$ is the Jacobian matrix obtained as $\boldsymbol{J}_o(\boldsymbol{q},s_o)=\delta i^+(s_c,s_o)/\delta s_o$ and $\boldsymbol{v}_o$ is the target velocity.

4. ADAPTIVE CONTROLLER

The following assumptions are considered, similar to those in references 6 and 12:

Assumption 4.1. *There exists $\boldsymbol{q}_d(t)$ such that the desired features vector $\boldsymbol{\xi}_d$ is achievable,*

$$\boldsymbol{\xi}_d=\boldsymbol{i}^+(s_c(\boldsymbol{q}_d(t)),s_o(t)).$$

Assmumption 4.2. *For the target path $s_o(t)$ there exists a neighborhood of $\boldsymbol{q}_d$ where $\boldsymbol{J}$ is bounded and invertible.*

Assumption 4.3. *The target velocity $\boldsymbol{v}_o$ is bounded.*

Now, we can formulate the tracking adaptive control problem for the robot with visual feedback.

4.1. Tracking control problem

Considering assumptions 4.1–4.3, desired features vector $\boldsymbol{\xi}_d$, initial estimates of dynamic parameters $\boldsymbol{\theta}$ in (3.2), initial estimates of target velocity $\hat{\boldsymbol{v}}_o$ and its derivative $d\hat{\boldsymbol{v}}_o/dt$, find, a control law,

$$\boldsymbol{\tau}=\boldsymbol{T}(\boldsymbol{q},\dot{\boldsymbol{q}},\boldsymbol{\xi},\hat{\boldsymbol{\theta}},\hat{\boldsymbol{v}}_o,d\hat{\boldsymbol{v}}_o/dt,t), \quad (8)$$

and a parameter update-law,

$$\frac{d}{dt}\hat{\boldsymbol{\theta}}=\boldsymbol{\Theta}(\boldsymbol{q},\dot{\boldsymbol{q}},\boldsymbol{\xi},\hat{\boldsymbol{\theta}},\hat{\boldsymbol{v}}_o,d\hat{\boldsymbol{v}}_o/dt,t) \quad (9)$$

such that the control error in the image plane $\boldsymbol{\xi}_d-\boldsymbol{\xi}(t)$ is ultimately bounded by a sufficiently small ball $\boldsymbol{B}_r$.

4.2. Generalized impedance control problem

The problem presented in the above subsection can be modified to include generalized impedance control objectives. An asymptotic impedance control objective can be defined as,

$$\boldsymbol{\xi}_d-\boldsymbol{\xi}(t)\rightarrow -(\boldsymbol{M}_m\boldsymbol{p}^2+\boldsymbol{B}_b\boldsymbol{p}+\boldsymbol{K}_k)^{-1}\boldsymbol{F}(t) \quad (10)$$

with $t\rightarrow\infty$, where $\boldsymbol{p}=\frac{d(.)}{dt}$ is the derivative operator, $\boldsymbol{M}_m$, $\boldsymbol{B}_b$ and $\boldsymbol{K}_k$ are positive definite diagonal design matrices of order $2m\times 2m$. $\boldsymbol{F}(t)$ is a fictitious force defined in the image plane.

The impedance error is defined now as,

$$\tilde{\boldsymbol{\xi}}=(\boldsymbol{\xi}_d+\boldsymbol{\xi}_o(t))-\boldsymbol{\xi}(t)=\boldsymbol{\xi}_r(t)-\boldsymbol{\xi}(t) \quad (11)$$

with $\boldsymbol{\xi}_o(t)=-(\boldsymbol{M}_m\boldsymbol{p}^2+\boldsymbol{B}_b\boldsymbol{p}+\boldsymbol{K}_k)^{-1}\boldsymbol{F}(t)$ and $\boldsymbol{\xi}_r(t)=\boldsymbol{\xi}_d+\boldsymbol{\xi}_o(t)$. In this paper, instead of the ideal asymptotic convergence to zero (10), ultimately boundedness of $\tilde{\boldsymbol{\xi}}(t)$ is considered as the control objective.

When there is no interaction between the robot and its environment, this problem reduces to the tracking one defined in subsection 4.1.

4.3. Control and update laws

A manifold $\boldsymbol{\nu}$ is defined[9] in the image error space as,

$$\boldsymbol{\nu}=\frac{d\tilde{\boldsymbol{\xi}}}{dt}+\Lambda\tilde{\boldsymbol{\xi}}. \tag{12}$$

Target velocity $\boldsymbol{v}_o$ and its derivative $\frac{d\boldsymbol{v}_o(t)}{dt}$ can be estimated by means of a second order filter,

$$\hat{\boldsymbol{v}}_o(t)=\frac{b_o p}{p^2+b_1 p+b_o}\boldsymbol{s}_o(t)$$

$$\frac{d\hat{\boldsymbol{v}}_o}{dt}=\frac{b_o p^2}{p^2+b_1 p+b_o}\boldsymbol{s}_o(t). \tag{13}$$

Using $\hat{\boldsymbol{v}}_o$ instead of $\boldsymbol{v}_o$ in equation (7), an estimate of the target velocity in the image plane $\dot{\hat{\boldsymbol{\xi}}}$ is given as, $\frac{d\hat{\boldsymbol{\xi}}}{dt}=\boldsymbol{J}\dot{\boldsymbol{q}}+\boldsymbol{J}_o\hat{\boldsymbol{v}}_o$. Now, by substituting in (12), an estimate of $\boldsymbol{\nu}$ is obtained,

$$\hat{\boldsymbol{\nu}}=\frac{d\hat{\tilde{\boldsymbol{\xi}}}}{dt+\Lambda\tilde{\boldsymbol{\xi}}} \tag{14}$$

The following control law is proposed,

$$\boldsymbol{\tau}=\boldsymbol{K}\hat{\boldsymbol{\nu}}'+\boldsymbol{\phi}\hat{\boldsymbol{\theta}} \tag{15}$$

with,

$$\hat{\boldsymbol{\nu}}'=\boldsymbol{J}^{-1}\hat{\boldsymbol{\nu}}=\boldsymbol{J}^{-1}\dot{\boldsymbol{\xi}}_o(t)-\dot{\boldsymbol{q}}-\boldsymbol{J}^{-1}\boldsymbol{J}_o\hat{\boldsymbol{v}}_o+\boldsymbol{J}^{-1}\Lambda\tilde{\boldsymbol{\xi}}, \tag{16}$$

where, $\dot{\boldsymbol{\xi}}_o(t)=-p(\boldsymbol{M}_m p^2+\boldsymbol{B}_b p+\boldsymbol{K}_k)^{-1}\boldsymbol{F}(t)$ and

$\boldsymbol{\phi}(\boldsymbol{q},\dot{\boldsymbol{q}},\boldsymbol{\nu},\hat{\boldsymbol{v}}_o,\frac{d\hat{\boldsymbol{v}}_o}{dt})\hat{\boldsymbol{\theta}}$

$$\begin{aligned}\boldsymbol{\phi}\hat{\boldsymbol{\theta}}=\hat{\boldsymbol{H}}(\boldsymbol{q})\{&\dot{\boldsymbol{J}}^{-1}\hat{\boldsymbol{\nu}}-\boldsymbol{J}^{-1}\dot{\boldsymbol{J}}\dot{\boldsymbol{q}}-\boldsymbol{J}^{-1}\dot{\boldsymbol{J}}_o\hat{\boldsymbol{v}}_o+\boldsymbol{J}^{-1}\ddot{\boldsymbol{\xi}}_o\\&-\boldsymbol{J}^{-1}\boldsymbol{J}_o\frac{d\hat{\boldsymbol{v}}_o}{dt}-\boldsymbol{J}^{-1}\Lambda\boldsymbol{J}\dot{\boldsymbol{q}}-\boldsymbol{J}^{-1}\Lambda\boldsymbol{J}_o\hat{\boldsymbol{v}}_o\\&+\boldsymbol{J}^{-1}\Lambda\dot{\boldsymbol{\xi}}_o\}+\hat{\boldsymbol{C}}(\boldsymbol{q},\dot{\boldsymbol{q}})\{-\boldsymbol{J}^{-1}\boldsymbol{J}_o\hat{\boldsymbol{v}}_o\\&+\boldsymbol{J}^{-1}\Lambda\tilde{\boldsymbol{\xi}}+\boldsymbol{J}^{-1}\dot{\boldsymbol{\xi}}_o\}+\hat{\boldsymbol{g}}(\boldsymbol{q}),\end{aligned} \tag{17}$$

where: $\boldsymbol{K}$ and $\boldsymbol{\Lambda}$ are positive definite gain $(n\times n)$ matrices, $\hat{\boldsymbol{H}}(\boldsymbol{q})$, $\hat{\boldsymbol{C}}(\boldsymbol{q},\dot{\boldsymbol{q}})$ and $\hat{\boldsymbol{g}}(\boldsymbol{q})$ are the estimates of $\boldsymbol{H}(\boldsymbol{q})$, $\boldsymbol{C}(\boldsymbol{q},\dot{\boldsymbol{q}})$ and $\boldsymbol{g}(\boldsymbol{q})$, respectively. Parameterization of (15) is possible due to property 3.2.

To estimate $\boldsymbol{\theta}$, the following parameter update-law is considered, which is the σ-modification type,[13]

$$\frac{d}{dt}\hat{\boldsymbol{\theta}}=\boldsymbol{\Gamma}\boldsymbol{\phi}^T(\boldsymbol{q},\dot{\boldsymbol{q}},\hat{\boldsymbol{\nu}},\hat{\boldsymbol{v}}_o,\frac{d\hat{\boldsymbol{v}}_o}{dt})\hat{\boldsymbol{\nu}}'-\boldsymbol{L}\hat{\boldsymbol{\theta}}, \tag{18}$$

with $\boldsymbol{\Gamma}$ and $\boldsymbol{L}$ positive definite adaptation gain $p\times p$ matrices.

5. STABILITY ANALYSIS

Proposition 5.1. *Consider the control law (15) and the update law (18) in closed loop with the robot and camera models (2) and (6) with the assumptions 4.1–4.3. Then, there exists a neighborhood of $\boldsymbol{q}_d$ such that,*

a) $\tilde{\boldsymbol{\theta}}=\boldsymbol{\theta}-\hat{\boldsymbol{\theta}}\in L_\infty^p$.

b) $\hat{\boldsymbol{\nu}}'\in L_\infty^n \cap L_2^n$.

c) $\tilde{\boldsymbol{\xi}}(t)=(\boldsymbol{\xi}(t)-\boldsymbol{\xi}(t))$ *is ultimately bounded.*

Proof: The closed-loop system is obtained by combining (2) and (15),

$$\boldsymbol{K}\hat{\boldsymbol{\nu}}'+\boldsymbol{\phi}\hat{\boldsymbol{\theta}}=\boldsymbol{H}\ddot{\boldsymbol{q}}+\boldsymbol{C}\dot{\boldsymbol{q}}+\boldsymbol{g} \tag{19}$$

Using $\hat{\boldsymbol{\theta}}=\boldsymbol{\theta}-\tilde{\boldsymbol{\theta}}$ and equations (12) and (18) it yields,

$$\boldsymbol{K}\hat{\boldsymbol{\nu}}'-\boldsymbol{\phi}\tilde{\boldsymbol{\theta}}+\boldsymbol{H}\hat{\boldsymbol{D}}\boldsymbol{\nu}'+\boldsymbol{C}\hat{\boldsymbol{\nu}}'=\boldsymbol{0} \tag{20}$$

where $\hat{\boldsymbol{D}}\boldsymbol{\nu}'$ is the estimate of the $\boldsymbol{\nu}'$ time derivative. But, $\hat{\boldsymbol{D}}\boldsymbol{\nu}'=\boldsymbol{D}\hat{\boldsymbol{\nu}}'+\boldsymbol{\varepsilon}'$, with $\boldsymbol{\varepsilon}'=\boldsymbol{J}^{-1}\Lambda\boldsymbol{J}_o(\boldsymbol{v}_o-\hat{\boldsymbol{v}}_o)$, $\boldsymbol{v}_o-\hat{\boldsymbol{v}}_o=\boldsymbol{\varepsilon}_o$ the estimate error, and $\boldsymbol{D}\hat{\boldsymbol{\nu}}'$ the time derivative of $\hat{\boldsymbol{\nu}}'$.

Then,

$$\boldsymbol{H}\boldsymbol{D}\hat{\boldsymbol{\nu}}'=-(\boldsymbol{K}+\boldsymbol{C})\hat{\boldsymbol{\nu}}'+\boldsymbol{\phi}\tilde{\boldsymbol{\theta}}-\boldsymbol{\varepsilon} \tag{21}$$

where, $\boldsymbol{\varepsilon}=\boldsymbol{H}\boldsymbol{\varepsilon}'$.

Considering the local non-negative function of time,

$$V=\frac{1}{2}\hat{\boldsymbol{\nu}}'^T\boldsymbol{H}\hat{\boldsymbol{\nu}}'+\frac{1}{2}\tilde{\boldsymbol{\theta}}^T\boldsymbol{\Gamma}^{-1}\tilde{\boldsymbol{\theta}} \tag{22}$$

whose time derivative along the trajectories of (21), considering the parameter update-law (18), is

$$\begin{aligned}\dot{V}=&\hat{\boldsymbol{\nu}}'^T[-(\boldsymbol{K}+\boldsymbol{C})\hat{\boldsymbol{\nu}}'+\boldsymbol{\phi}\tilde{\boldsymbol{\theta}}-\boldsymbol{\varepsilon}]\\&+\frac{1}{2}\hat{\boldsymbol{\nu}}'^T\dot{\boldsymbol{H}}\hat{\boldsymbol{\nu}}'+\tilde{\boldsymbol{\theta}}\boldsymbol{\Gamma}^{-1}[-\boldsymbol{\Gamma}\boldsymbol{\phi}^T\hat{\boldsymbol{\nu}}+\boldsymbol{L}\hat{\boldsymbol{\theta}}].\end{aligned} \tag{23}$$

Considering property 3.1, it results,

$$\dot{V}=-\hat{\boldsymbol{\nu}}'^T\boldsymbol{K}\hat{\boldsymbol{\nu}}'-\tilde{\boldsymbol{\theta}}^T\boldsymbol{\Gamma}^{-1}\boldsymbol{L}\tilde{\boldsymbol{\theta}}-\hat{\boldsymbol{\nu}}'\boldsymbol{\varepsilon}+\tilde{\boldsymbol{\theta}}^T\boldsymbol{\Gamma}^{-1}\boldsymbol{L}\boldsymbol{\theta}. \tag{24}$$

Using the expressions,

$$\|\tilde{\boldsymbol{\theta}}\|\|\boldsymbol{\theta}\|\le\frac{1}{2}\frac{1}{\delta^2}\|\tilde{\boldsymbol{\theta}}\|^2+\frac{\delta^2}{2}\|\boldsymbol{\theta}\|^2$$

$$\|\hat{\boldsymbol{\nu}}'^T\|\|\boldsymbol{\varepsilon}\|\le\frac{1}{2\eta^2}\|\hat{\boldsymbol{\nu}}'\|^2+\frac{\eta^2}{2}\|\boldsymbol{\varepsilon}\|^2 \tag{25}$$

with $\delta,\eta\in\mathrm{IR}^+$, the equation (24) can be expressed as,

$$\begin{aligned}\dot{V}\le&-\mu_K\|\hat{\boldsymbol{\nu}}'\|^2-\mu_{\Gamma^{-1}L}\|\tilde{\boldsymbol{\theta}}\|^2\\&+\|\hat{\boldsymbol{\nu}}'\|\|\boldsymbol{\varepsilon}\|+\gamma_{\Gamma^{-1}L}\|\boldsymbol{\theta}\|\tilde{\boldsymbol{\theta}}\|\end{aligned} \tag{26}$$

with $\mu_K=\sigma_{\min}(\boldsymbol{K})$, $\mu_{\Gamma^{-1}L}=\sigma_{\min}(\boldsymbol{\Gamma}^{-1}\boldsymbol{L})$ and $\gamma_{\Gamma^{-1}L}=\sigma_{\max}(\boldsymbol{\Gamma}^{-1}\boldsymbol{L})$, where σ denotes singular value.

Also,

$$\dot{V}=-\alpha_1\|\hat{\boldsymbol{\nu}}'\|^2-\alpha_2\|\tilde{\boldsymbol{\theta}}\|^2+\rho \tag{27}$$

where,

$$\alpha_1=\mu_K-\frac{1}{2\eta^2}>0$$

$$\alpha_2=\mu_{\Gamma^{-1}L}-\frac{\gamma_{\Gamma^{-1}L}}{2\delta^2}>0 \tag{28}$$

$$\rho=\gamma_{\Gamma^{-1}L}\frac{\delta^2}{2}\|\boldsymbol{\theta}\|^2+\frac{\eta^2}{2}\|\boldsymbol{\varepsilon}\|^2.$$

Equation (22) can be upper bounded by,

$$V=\beta_1\|\hat{\boldsymbol{\nu}}'\|^2+\beta_2\|\tilde{\boldsymbol{\theta}}\|^2 \tag{29}$$

where, $\beta_1=\frac{1}{2}\gamma_H$, with $\gamma_H=\sup_q[\sigma_{\max}(\boldsymbol{H})]$ and $\gamma_{\Gamma^{-1}}=\sigma_{\max}(\boldsymbol{\Gamma}^{-1})$.

Then,

$$\dot{V}\leq-\gamma V+\rho \tag{30}$$

with, $\gamma=\min\{\frac{\alpha_1}{\beta_1},\frac{\alpha_2}{\beta_2}\}$.

As ρ is bounded, equation (30) implies $\hat{\boldsymbol{\nu}}'\in L_\infty^{2n}$, $\tilde{\boldsymbol{\theta}}\in L_\infty^{p}$ which proves *(a)* and *(b)*. Also, $\boldsymbol{x}=(\hat{\boldsymbol{\nu}}',\tilde{\boldsymbol{\theta}})^T$ is ultimately bounded inside a ball $\boldsymbol{B}(\boldsymbol{0},\mathbf{r})$. Now, from (12), $\hat{\boldsymbol{\nu}}=\boldsymbol{J}\hat{\boldsymbol{\nu}}'$ and by assumption 4.2, $\hat{\boldsymbol{\nu}}'\in L_\infty^{2m}$. Note that, $\hat{\boldsymbol{\nu}}$ can be expressed in terms of $\boldsymbol{\nu}$ as,

$$\hat{\boldsymbol{\nu}}=\frac{d\tilde{\boldsymbol{\xi}}}{dt}+\boldsymbol{\Lambda}\tilde{\boldsymbol{\xi}}+\boldsymbol{J}_o(\boldsymbol{v}_o-\hat{\boldsymbol{v}}_o)=\boldsymbol{\nu}+\boldsymbol{J}_o\boldsymbol{\varepsilon}_o. \tag{31}$$

As $\boldsymbol{J}_o\boldsymbol{\varepsilon}_o$ is bounded, it means that $\boldsymbol{\nu}$ is ultimately bounded.[14] From the last equation, $\tilde{\boldsymbol{\xi}}=\boldsymbol{O}(\boldsymbol{\nu})$ where, $\boldsymbol{O}(\cdot)$ is a linear operator with finite gain. Therefore, $\|\tilde{\boldsymbol{\xi}}\|=\|\boldsymbol{O}\|\|\boldsymbol{\nu}\|$ then, as $\boldsymbol{\nu}$ is ultimately bounded $\tilde{\boldsymbol{\xi}}$ is also ultimately bounded, which proves *(c)*. Consequently, $\boldsymbol{\xi}_r(t)-\boldsymbol{\xi}(t)$ is ultimately bounded. The last, implies that if the object is placed at a distance greater than $|\boldsymbol{r}|$ ($\boldsymbol{\xi}_o\equiv\boldsymbol{0}$) it is verified that $\boldsymbol{\xi}_o-\boldsymbol{\xi}(t)$ is ultimately bounded, which implies that the tracking control objective is satisfied.

Remark 1: If more features than degrees of freedom of the robot are taken, a non-square Jacobian matrix is obtained. In this case a redefinition of $\boldsymbol{\nu}$ as, $\boldsymbol{\nu}=\frac{d(\boldsymbol{J}^T\tilde{\boldsymbol{\xi}})}{dt}+\boldsymbol{\Lambda}(\boldsymbol{J}^T\tilde{\boldsymbol{\xi}})$, must be used. Reasoning in a similar way as in proposition above, it is possible to reach the same conclusions about the behaviour of the control system.

Remark 2: It is possible to calculate a bound for the ultimately behaviour of the control errors. This bound of control errors depends on controller gains, the object velocity estimation error and the inertia matrix of the robot.

6. SIMULATIONS

Computer simulations have been carried out to show the stability and performance of the proposed tracking adaptive impedance controller. The manipulator used for the simulations is two-degree-of-freedom manipulator, as shown in Figure 1. The meaning and numerical values of the symbols are listed in Table I.

The elements $\boldsymbol{H}_{ij}(\boldsymbol{q})(i,j=1,2)$ of the inertia matrix $\boldsymbol{H}(\boldsymbol{q})$ are,

$$H_{11}(\boldsymbol{q})=m_1l_{c1}^2+m_2(l_1^2+l_{c2}^2+2l_1l_{c2}\cos(q_2))$$
$$+I_1+I_2$$
$$H_{12}(\boldsymbol{q})=m_2l_{c2}^2+l_1l_{c2}\cos(q_2))+I_2$$
$$H_{21}(\boldsymbol{q})=m_2(l_{c2}^2+l_1l_{c2}\cos(q_2))+I_2$$
$$H_{22}(\boldsymbol{q})=m_2l_{c2}^2+I_2.$$

The elements $\boldsymbol{C}_{ij}(\boldsymbol{q},\dot{\boldsymbol{q}})(i,j=1,2)$ from the centrifugal and Coriolis matrix $\boldsymbol{C}(\boldsymbol{q},\dot{\boldsymbol{q}})$ are,

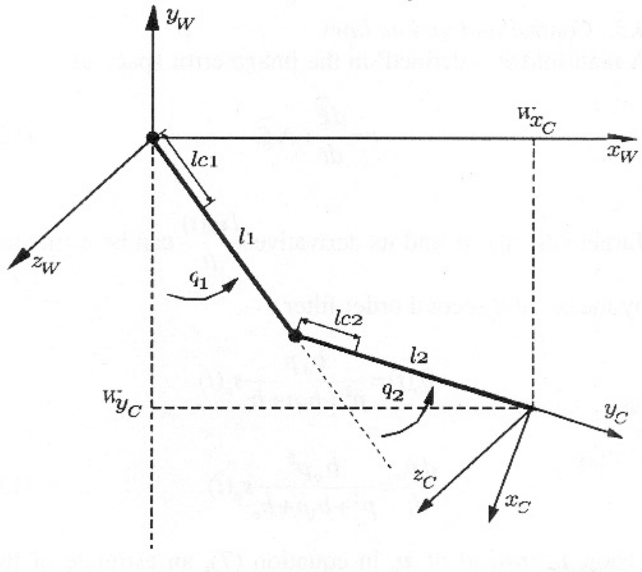

Fig. 1. Direct drive 2 d.o.f. manipulator.

$$C_{11}(\boldsymbol{q},\dot{\boldsymbol{q}})=-m_2l_1l_{c2}\sin(q_2)\dot{q}_2$$
$$C_{12}(\boldsymbol{q},\dot{\boldsymbol{q}})=-m_2l_1l_{c2}\sin(q_2)(\dot{q}_1+\dot{q}_2)$$

Table I. Manipulator parameters

	notation	value	units
Length link 1	l_1	0.45	m
Length link 2	l_2	0.55	m
C. of G., link 1	l_{c1}	0.091	m
C. of G., link 2 + camera	l_{c2}	0.105	m
Mass link 1	m_1	23.9	kg
Mass link 2 + camera	m_2	4.44	kg
Inertia link 1	I_1	1.27	Kg m^2
Inertia link 2 + camera	I_2	0.24	Kg m^2

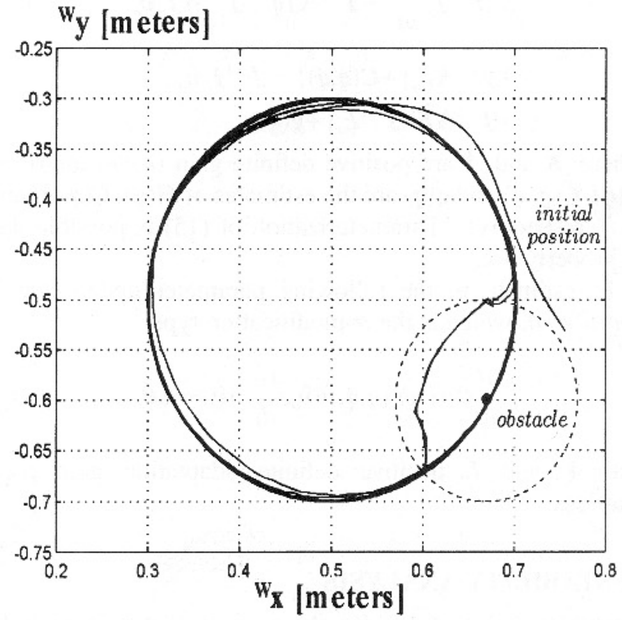

Fig. 2. End-effector trajectory in the work space.

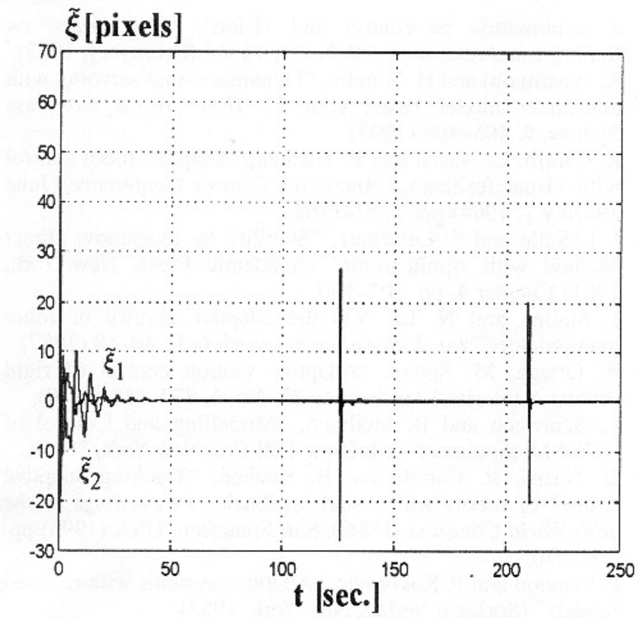

Fig. 3. Evolution of the control error.

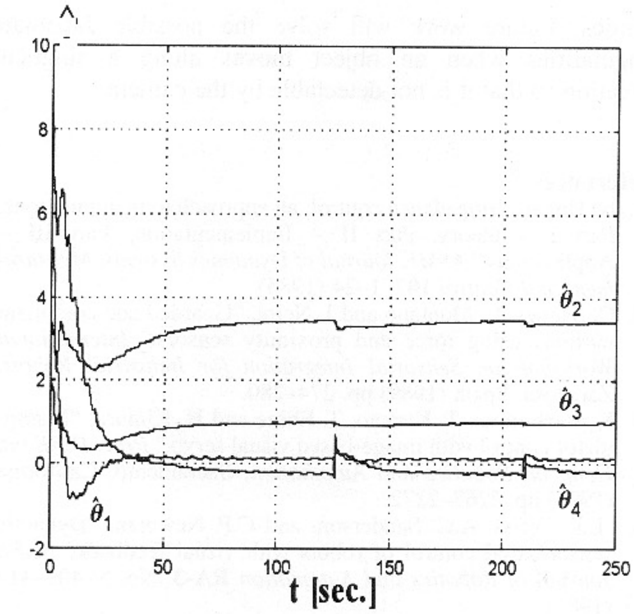

Fig. 4. Evolution of the parameters.

$$C_{21}(\boldsymbol{q},\dot{\boldsymbol{q}})=m_2 l_1 l_{c2}\sin(q_2)\dot{q}_1$$

$$C_{22}(\boldsymbol{q},\dot{\boldsymbol{q}})=0.$$

The entries of the gravitational torque vector $\boldsymbol{g(q)}$ are given by,

$$g_1(\boldsymbol{q})=(m_1 l_{c1}+m_2 l_1)g\sin(q_1)+m_2 l_{c2} g\sin(q_1+q_2)$$

$$g_2(\boldsymbol{q})=m_2 l_{c2} g\sin(q_1+q_2).$$

The numerical values of the camera model are *focal length* $f = 0.008m$ and the *scale factor* $\alpha = 72727$ *pixels/m*.

The linear parameterization of equation (15) leads to a parameter vector

$$\boldsymbol{\theta}=[m_1 l_{c1}^2 \quad m_1 l_{c1} \quad m_2 l_{c2}^2 \quad m_2 l_{c2} \quad m_2 \quad I_1 \quad I_2]^T.$$

For controller design it is assumed that the values are known with uncertainties of about 40%. Simulations are carried out using the following design parameters $\boldsymbol{\Lambda} = diag(\lambda)$, $\lambda_i = 15$, $\boldsymbol{K} = diag(k)$, $k_i = 100$ and $\boldsymbol{\Gamma} = diag(\gamma)$, $\gamma_i = 0.9$ and $\boldsymbol{L} = diag(l_i)$, $l_i = .00025$.

The robot initial conditions are $q_1(0) = 30°$, $q_2 = 45°$, $\dot{q}_1 = 0$ and $\dot{q}_2 = 0$. The parameters of desired impedance are $\boldsymbol{M}_m = diag(0.01)$, $\boldsymbol{B}_b = diag(1)$ and $\boldsymbol{K}_k = diag(30)$.

The trajectory of the object is a circle with radius $rd = 0.2m$, angular velocity $\omega = 1.05 rad/sec$ and the parameters of the second order filters are, $b_o = 4\,10^4$, $b_1 = 400$.

The desired image feature point was set to $\boldsymbol{\xi}_d = [0 \quad 0]^T$. The obstacle is considered circular and its center in $[0.67m \quad -0.6m]^T$ within work space of the robot. The distance to which the fictitious force begin to act is $r = 0.1m$.

Simulation results are shown in Figures 2 to 5. Figure 2 shows the end-effector trajectory in the work plane. Figure 3 shows evolutions of the control errors $\tilde{\boldsymbol{\xi}}$. Finally, in the Figures 4 and 5 are shown the parameters of the robot.

7. CONCLUSIONS

In this paper, we presented a tracking adaptive impedance controller for robots with camera-in-hand configuration using visual feedback, in which a generalized impedance concept has been used in order to avoid obstacles. Full non-linear robot dynamics has been considered in the controller design. The control errors are proved to be ultimately bounded. Simulations illustrate the ability of the proposed controller to attain accurate control under dynamics uncer-

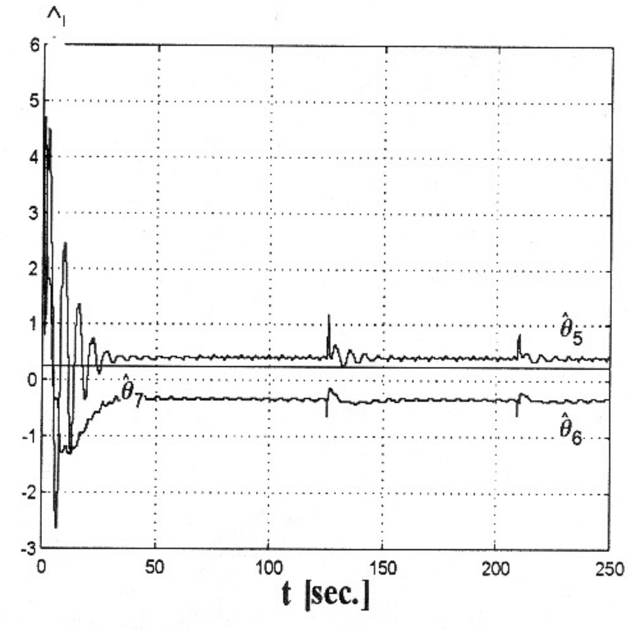

Fig. 5. Evolution of the parameters.

tainties. Future work will solve the possible Jacobian singularities when an object moves along a singular direction so that it is not detectable by the camera.

References

1. N. Hogan, "Impedance control: an approach to manipulations, Part I – theory, Part II – Implementation, Part III – Applications," *ASME Journal of Dynamics Systems, Measurement and Control* **107**, 1–24 (1985).
2. C. Sagues, L. Montano and J. Neira, "Guarded and compliant motions using force and proximity sensors," *International Workshop on Sensorial Integration for Industrial Robots*, Zaragosa, Spain (1989) pp. 274–280.
3. K. Hashimoto, T. Kimoto, T. Ebine and H. Kimura, "Manipulator control with image-based visual servo," *Proc. IEEE int. Conf. on Robotics and Automation*, Sacramento, California (1991) pp. 2267–2272.
4. L.E. Weiss, A.C. Sanderson, and C.P. Newman, "Dynamic sensor-based control of robots with visual feedback," *IEEE Journal of Robotics and Automation* **RA-3**, No. 5, 409–417 (1987).
5. N.P. Papanikolopoulos, P.K. Khosla and T. Kanade, "Visual tracking of a moving target by a camera mounted on a robot: a combination of control and vision," *IEEE Trans. on Robotics and Automation* **9**, No. 1, 14–34 (Februyary, 1993).
6. K. Hashimoto and H. Kimura, "Dynamic visual servoing with non-linear model based control," *IFAC World Congress* Sydney, **9**, 405–408 (1993).
7. R. Carelli, O. Nasisi and B. Kuchen, "Adaptive robot control with visual feedback," *American Control Conference* (June 29–July 1, 1994) pp. 1757–1762.
8. J. LaSalle and S. Lefschetz, "Stability by Lyapunov: Direct Method with Applications" (Academic Press, New York, 1961) Chapter 4, pp. 107–130.
9. J. Slotine and N. Li, "On the adaptive control of robot manipulators," *Int. J. Robotics Research* **6**(3), 49–59 (1987).
10. R. Ortega, M. Spong, "Adaptive motion control of rigid robots: A tutorial," *Automatica* **25**, No. 6, 877–888 (1989).
11. L. Sciavicco and B. Siciliano, "Modelling and Control of Robot Manipulators" (McGraw-Hill Co., New York, 1996).
12. O. Nasisi, R. Carelli and B. Kuchen, "Tracking adaptive control of robots with visual feedback," *Proceedings of the 13th World Congress (IFAC)*, San Francisco, USA (1996) pp. 265–270.
13. P. Ioannou and P. Kokotovic, "Adaptive systems with reduced models" (Springer Verlag, New York, 1983).
14. C. Desoer and M. Vidyasagar, "Feedback systems: Input-Output properties" (Academic Press, New York, 1975).